Appears in the Proceedings of IST'07, July 2007.

3-D MIMO Mobile-to-Mobile Channel Simulation

Alenka G. Zajić and Gordon L. Stüber
School of Electrical and Computer Engineering
Georgia Institute of Technology, Atlanta, GA 30332 USA

***Abstract*— Mobile-to-mobile (M-to-M) radio propagation channels arise in inter-vehicular communications, mobile ad-hoc wireless networks, and relay-based cellular radio networks. The statistical properties of M-to-M channels are quite different from conventional fixed-to-mobile (F-to-M) cellular land mobile radio channels. This article presents a 3-D mathematical reference model for multiple-input multiple-output (MIMO) M-to-M channels. Based on this model, a sum-of-sinusoids based simulation model is proposed for 3-D MIMO M-to-M multipath-fading channels, along with simplified deterministic and statistical models for 2-D non-isotropic scattering. The statistics of the simulation models are verified by simulation.**

I. Introduction

Mobile-to-mobile (M-to-M) communications play an important role in mobile ad-hoc wireless networks, intelligent transportation systems, and relay-based cellular networks. M-to-M communication systems are equipped with low elevation antennas and have both the transmitter ($\mathrm{T_x}$) and the receiver ($\mathrm{R_x}$) in motion. To successfully design M-to-M systems, it is necessary to have a detailed knowledge of the outdoor multipath fading channel and its statistical properties. Early studies of single-input single-output (SISO) M-to-M Rayleigh fading channels have been reported by Akki & Haber in [1], [2]. They showed that the received envelope of M-to-M channels is Rayleigh faded under non line-of-sight conditions, but the statistical properties differ from fixed-to-mobile (F-to-M) channels. They also proposed a reference model for SISO M-to-M Rayleigh fading channels. Simulation models for SISO M-to-M channels have been proposed in [3]-[5]. Recently, the reference models for narrowband multiple-input multiple-output (MIMO) M-to-M channels have been proposed [6], [7], and corresponding simulation models in [8], [9].

All previously reported models assume that the field incident on the $\mathrm{T_x}$ or the $\mathrm{R_x}$ antenna is composed of a number of waves travelling only in the *horizontal* plane. This assumption is acceptable only for certain environments, e.g., rural areas. However, it does not seem appropriate for an urban environment where the $\mathrm{T_x}$ and $\mathrm{R_x}$ antenna arrays are often located in close proximity to, and lower than, the surrounding buildings. Scattered waves may propagate by diffraction from the edges of buildings down to the street and, thus, not necessarily travel horizontally. To overcome these shortcomings, this paper proposes a three-dimensional (3-D) reference model for MIMO M-to-M multipath fading channels. To describe our 3-D reference model, we first introduce a 3-D geometrical model for MIMO M-to-M channels, referred to as a "two-cylinder" model. This model is extension of the one-cylinder model for F-to-M channels proposed in [10], [11]. By taking into account local scattering around both the $\mathrm{T_x}$ and $\mathrm{R_x}$, and by including mobility of both the $\mathrm{T_x}$ and $\mathrm{R_x}$, we obtain our two-cylinder model. The reference model assumes an infinite number of scatterers, which prevents practical implementation. Hence, we propose deterministic and statistical SoS simulation models for a 3-D non-isotropic scattering environment. The statistical properties of our model are derived and verified by simulations.

The remainder of this paper is organized as follows. Section II introduces a geometrical two-cylinder model. Section III presents a 3-D reference model for MIMO M-to-M channels. Section V presents the deterministic and statistical 3-D SoS simulation models along with some representative simulation results. Finally, Section VI provides some concluding remarks.

[0] Prepared through collaborative participation in the Collaborative Technology Alliance for Communications & Networks sponsored by the U.S. Army Research Laboratory under Cooperative Agreement DAAD19-01-2-0011. The U.S. Government is authorized to reproduce and distribute reprints for Government purposes notwithstanding any copyright notation thereon.

II. A Geometrical Two-Cylinder Model

In this section, we introduce a 3-D geometrical model for MIMO M-to-M channels, called a two-cylinder model. The two-cylinder model is an extension of the one-cylinder model for F-to-M channels proposed in [10], [11]. We consider a narrow-band MIMO communication system with L_t transmit and L_r receive omnidirectional antenna elements. It is assumed that both the $\mathrm{T_x}$ and $\mathrm{R_x}$ are in motion and equipped with low elevation antennas. The radio propagation environment is characterized by 3-D scattering with non-line-of-sight (NLoS) propagation conditions between the $\mathrm{T_x}$ and $\mathrm{R_x}$. By taking into account local scattering around both the $\mathrm{T_x}$ and $\mathrm{R_x}$ and by including mobility of both the $\mathrm{T_x}$ and $\mathrm{R_x}$, we obtain our two-cylinder model.

Fig. 1 shows the two-cylinder model for a MIMO M-to-M channel with $L_t = L_r = 2$ antenna elements. The two-cylinder model defines two cylinders, one around the $\mathrm{T_x}$ and another around the $\mathrm{R_x}$, as shown in Fig. 1. Around the transmitter, M fixed omnidirectional scatterers lie on a surface of a cylinder of radius R_t, and the m^{th} transmit scatterer is denoted by $S_T^{(m)}$. Similarly, around the receiver, N fixed omnidirectional scatterers lie on the surface of a cylinder of radius R_r, and the n^{th} receive scatterer is denoted by $S_R^{(n)}$. The distance between the centers of the $\mathrm{T_x}$ and $\mathrm{R_x}$ cylinders is D. It is assumed that the radii R_t and R_r are much smaller than the distance D, i.e., $\max\{R_t, R_r\} \ll D$. The spacing between antenna elements at the $\mathrm{T_x}$ and $\mathrm{R_x}$ is denoted by d_T and d_R, respectively. It is assumed that d_T and d_R are much smaller than the radii R_t and R_r, i.e., $\max\{d_T, d_R\} \ll \min\{R_t, R_r\}$. Angles θ_T and θ_R describe the orientation of the $\mathrm{T_x}$ and $\mathrm{R_x}$

antenna array in the x-y plane, respectively, relative to the y-axis. Similarly, angles ψ_T and ψ_R describe the elevation of the $\mathrm{T_x}$'s antenna array and the $\mathrm{R_x}$'s antenna array relative to the x-y plane, respectively. The $\mathrm{T_x}$ and $\mathrm{R_x}$ are moving with speeds v_T and v_R in directions described by angles γ_T and γ_R, respectively. The symbols $\alpha_T^{(m)}$ and $\alpha_R^{(n)}$ denote the azimuth angle of departure (AAoD) and the azimuth angle of arrival (AAoA), respectively. Similarly, the symbols $\beta_T^{(m)}$ and $\beta_R^{(n)}$ denote the elevation angle of departure (EAoD) and the elevation angle of arrival (EAoA), respectively. Finally, the symbols ϵ_{pm}, ϵ_{mn}, and ϵ_{nq} denote distances $A_T^{(p)}$–$S_T^{(m)}$, $S_T^{(m)}$–$S_R^{(n)}$, and $S_R^{(n)}$–$A_R^{(q)}$, respectively, as shown in Fig. 1.

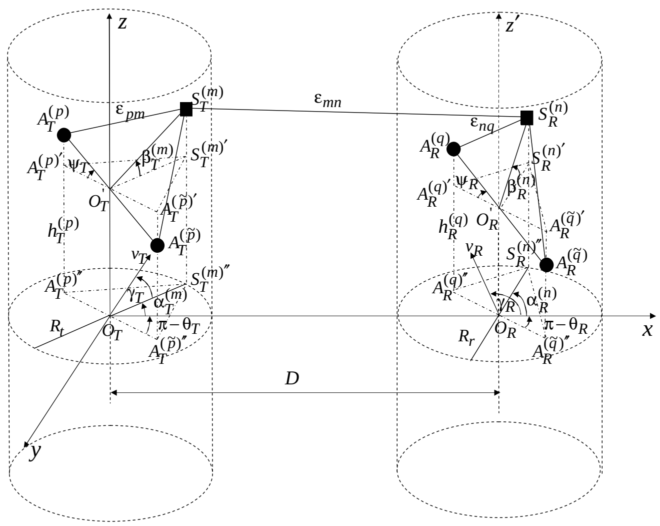

Fig. 1. The two-cylinder model for MIMO M-to-M channel with $L_t = L_r = 2$ antenna elements.

III. A 3-D Reference Model for MIMO Mobile-to-Mobile Channels

This section outlines a reference model for MIMO M-to-M multipath fading channels. The starting point is the two-cylinder model shown in Fig. 1. From the two-cylinder model, we observe that the waves from the $\mathrm{T_x}$ antenna elements impinge on the scatterers located on the $\mathrm{T_x}$ cylinder and scatter from the scatterers located on the $\mathrm{R_x}$ cylinder before they arrive at the $\mathrm{R_x}$ antenna elements. In contrast to cellular F-to-M channels where waves are single-bounced, in M-to-M channels waves are double-bounced.

The MIMO channel is described by an $L_r \times L_t$ matrix $\mathbf{H}(t) = [h_{ij}(t)]_{L_r \times L_t}$ of complex low-pass faded envelopes. In the 3-D reference model, the number of local scatterers around the $\mathrm{T_x}$ and $\mathrm{R_x}$ is infinite. Consequently, the received complex faded envelope of the link $A_T^{(p)} - A_R^{(q)}$ is

$$h_{pq}(t) = \lim_{M,N\to\infty} \sqrt{\frac{1}{MN}} \sum_{m=1}^{M} \sum_{n=1}^{N} e^{-j\frac{2\pi}{\lambda}(\epsilon_{pm}+\epsilon_{mn}+\epsilon_{nq})+j\phi_{mn}} e^{j2\pi t[f_{T\max}\cos(\alpha_T^{(m)}-\gamma_T)\cos\beta_T^{(m)}+f_{R\max}\cos(\alpha_R^{(n)}-\gamma_R)\cos\beta_R^{(n)}]}, \quad (1)$$

where $f_{T\max} = v_T/\lambda$ and $f_{R\max} = v_R/\lambda$ are the maximum Doppler frequencies associated with the $\mathrm{T_x}$ and $\mathrm{R_x}$, respectively, and λ is the carrier wavelength. It is assumed that the angles of departures (AAoDs and EAoDs) and the angles of arrivals (AAoAs and EAoAs) are random variables, and that the angles of departure are independent from the angles of arrival. Additionally, it is assumed that the phases ϕ_{mn} are random variables uniformly distributed on the interval $[-\pi, \pi)$ and independent from the angles of departure and the angles of arrival.

The distances ϵ_{pm}, ϵ_{mn}, and ϵ_{nq} can be expressed as functions of the random variables $\alpha_T^{(m)}$, $\alpha_R^{(n)}$, $\beta_T^{(m)}$, and $\beta_R^{(n)}$ as follows:

$$\epsilon_{pm} \approx R_t - \frac{d_T}{2}\sin\psi_T \sin\beta_T^{(m)} - \frac{d_T}{2}\cos\psi_T\cos\beta_T^{(m)}\left(\cos\theta_T\cos\alpha_T^{(m)} + \sin\theta_T\sin\alpha_T^{(m)}\right), \quad (2)$$

$$\epsilon_{nq} \approx R_r - \frac{d_R}{2}\sin\psi_R \sin\beta_R^{(n)} - \frac{d_R}{2}\cos\psi_R\cos\beta_R^{(n)}\left(\cos\theta_R\cos\alpha_R^{(n)} + \sin\theta_R\sin\alpha_R^{(n)}\right), \quad (3)$$

$$\epsilon_{mn} \approx D. \quad (4)$$

Derivations of (2) - (4) are omitted for brevity.

Using (2) - (4), the complex faded envelope of the link $A_T^{(p)} - A_R^{(q)}$ can be rewritten as

$$h_{pq}(t) = \lim_{M,N\to\infty} \frac{1}{\sqrt{MN}} \sum_{m,n=1}^{M,N} a_{p,m} b_{n,q} e^{j\phi_{mn}+j\phi_0} e^{j2\pi t[f_{T\max}\cos(\alpha_T^{(m)}-\gamma_T)\cos\beta_T^{(m)}+f_{R\max}\cos(\alpha_R^{(n)}-\gamma_R)\cos\beta_R^{(n)}]}, \quad (5)$$

where $\phi_0 = -2\pi\left(R_t + R_r + D\right)/\lambda$ and parameters $a_{p,m}$ and $b_{n,q}$ are defined as

$$\begin{aligned} a_{p,m} &= e^{j\frac{\pi}{\lambda}d_T\sin\psi_T\sin\beta_T^{(m)}} \\ &\times e^{j\frac{\pi}{\lambda}d_T\cos\psi_T\cos\beta_T^{(m)}(\cos\theta_T\cos\alpha_T^{(m)}+\sin\theta_T\sin\alpha_T^{(m)})}, \end{aligned} \quad (6)$$

$$\begin{aligned} b_{n,q} &= e^{j\frac{\pi}{\lambda}d_R\sin\psi_R\sin\beta_R^{(n)}} \\ &\times e^{j\frac{\pi}{\lambda}d_R\cos\psi_R\cos\beta_R^{(n)}(\cos\theta_R\cos\alpha_R^{(n)}+\sin\theta_R\sin\alpha_R^{(n)})}. \end{aligned} \quad (7)$$

Note that the constant phase ϕ_0 can be set to zero without loss of generality because it does not affect statistical properties of the model.

IV. Space-Time Correlation Function of the 3-D Reference Model

The normalized space-time correlation function between two complex faded envelopes $h_{pq}(t)$ and $h_{\tilde{p}\tilde{q}}(t)$ is

$$R_{pq,\tilde{p}\tilde{q}}[d_T, d_R, \tau] \triangleq \frac{\mathrm{E}\left[h_{pq}(t)h^*_{\tilde{p}\tilde{q}}(t+\tau)\right]}{\sqrt{\mathrm{E}[|h_{pq}(t)|^2]\mathrm{E}[|h_{\tilde{p}\tilde{q}}(t)|^2]}}, \quad (8)$$

where $(\ \cdot\ )^*$ denotes complex conjugate operation, $\mathrm{E}[\ \cdot\ ]$ is the statistical expectation operator, $p, \tilde{p} \in \{1, \ldots L_t\}$, and

$q, \tilde{q} \in \{1, \ldots L_r\}$. Using (5) and (8), the space-time correlation function can be written as

$$R_{pq,\tilde{p}\tilde{q}}[d_T, d_R, \tau] = \lim_{M,N\to\infty} \frac{1}{MN} \sum_{m,n=1}^{M,N} \mathrm{E}\Big[a_{p,m} b_{n,q} a^*_{\tilde{p},m} b^*_{n,\tilde{q}} \tag{9}$$
$$e^{-j2\pi\tau \quad f_{T\max}\cos(\alpha_T^{(m)} - \gamma_T)\cos\beta_T^{(m)} + f_{R\max}\cos(\alpha_R^{(n)} - \gamma_R)\cos\beta_R^{(n)}} \Big].$$

Since the number of local scatterers in the reference model described in Section III is infinite, the discrete AAoDs, $\alpha_T^{(m)}$, EAoDs, $\beta_T^{(m)}$, AAoAs, $\alpha_R^{(n)}$, and EAoAs, $\beta_R^{(n)}$, can be replaced with continuous random variables α_T, β_T, α_R, and β_R having probability density functions (pdf) $f(\alpha_T)$, $f(\beta_T)$, $f(\alpha_R)$, and $f(\beta_R)$, respectively. Hence, (9) becomes

$$\begin{aligned} R_{pq,\tilde{p}\tilde{q}}[d_T, d_R, \tau] = & \int_{-\beta_{R_m}}^{\beta_{R_m}} \int_{-\beta_{T_m}}^{\beta_{T_m}} \int_{-\pi}^{\pi} \int_{-\pi}^{\pi} f(\alpha_T) f(\beta_T) f(\alpha_R) f(\beta_R) \\ & e^{-j2\pi\tau f_{T\max}\cos(\alpha_T - \gamma_T)\cos\beta_T + j\frac{2\pi}{\lambda} d_T \sin\psi_T \sin\beta_T} \\ & e^{j\frac{2\pi}{\lambda} d_T \cos\psi_T \cos\beta_T \cos\theta_T \cos\alpha_T + j\frac{2\pi}{\lambda} d_T \cos\psi_T \cos\beta_T \sin\theta_T \sin\alpha_T} \\ & e^{-j2\pi\tau f_{R\max}\cos(\alpha_R - \gamma_R)\cos\beta_R + j\frac{2\pi}{\lambda} d_R \sin\psi_R \sin\beta_R} \\ & e^{j\frac{2\pi}{\lambda} d_R \cos\psi_R \cos\beta_R (\cos\theta_R \cos\alpha_R + \sin\theta_R \sin\alpha_R)} d\alpha_T d\beta_T d\alpha_R d\beta_R, \end{aligned} \tag{10}$$

where β_{T_m} and β_{R_m} are the maximum elevation angles of the scatterers around the $\mathrm{T_x}$ and $\mathrm{R_x}$, respectively.

Several different scatterer distributions, such as uniform, Gaussian, Laplacian, and von Mises, are used in prior work to characterize the continuous random variables α_T and α_R. In this paper, we use the von Mises pdf because it approximates many of the aforementioned distributions and leads to closed-form solutions for many useful situations. The von Mises pdf is defined as [12]

$$f(\theta) \triangleq \frac{1}{2\pi I_0(k)} \exp\left[k\cos(\theta - \mu)\right], \tag{11}$$

where $\theta \in [-\pi, \pi)$, $I_0(\ \cdot\ )$ is the zeroth-order modified Bessel function of the first kind, $\mu \in [-\pi, \pi)$ is the mean angle at which the scatterers are distributed in the x - y plane, and k controls the spread of scatterers around the mean. To characterize the continuous random variables β_T and β_R, we use the pdf [11]

$$f(\varphi) = \begin{cases} \frac{\pi}{4|\varphi_m|}\cos\left(\frac{\pi}{2}\frac{\varphi}{\varphi_m}\right) & , \quad |\varphi| \le |\varphi_m| \le \frac{\pi}{2} \\ 0 & , \quad \text{otherwise} \end{cases}, \tag{12}$$

where φ_m is the maximum elevation angle and takes values in the range $10^\circ \le |\varphi_m| \le 20^\circ$ [13].

As shown in [14], the space-time correlation function in (10) can be closely approximated as

$$\begin{aligned} R_{pq,\tilde{p}\tilde{q}}[d_T, d_R, \tau] \approx & \frac{I_0(\sqrt{x^2+y^2})\cos\left(\frac{2\pi}{\lambda}\beta_{T_m} d_T \sin\psi_T\right)}{I_0(k_T)\left[1 - \left(\frac{4\beta_{T_m} d_T \sin\psi_T}{\lambda}\right)^2\right]} \\ & \times \frac{I_0(\sqrt{w^2+z^2})\cos\left(\frac{2\pi}{\lambda}\beta_{R_m} d_R \sin\psi_R\right)}{I_0(k_R)\left[1 - \left(\frac{4\beta_{R_m} d_R \sin\psi_R}{\lambda}\right)^2\right]}, \end{aligned} \tag{13}$$

where parameters x, y, z, and w are

$$\begin{aligned} x &= j2\pi d_{T_x}/\lambda - j2\pi\tau f_{T\max}\cos\gamma_T + k_T\cos\mu_T, \\ y &= j2\pi d_{T_y}/\lambda - j2\pi\tau f_{T\max}\sin\gamma_T + k_T\sin\mu_T, \\ z &= j2\pi d_{R_x}/\lambda - j2\pi\tau f_{R\max}\cos\gamma_R + k_R\cos\mu_R, \\ w &= j2\pi d_{R_y}/\lambda - j2\pi\tau f_{R\max}\sin\gamma_R + k_R\sin\mu_R, \end{aligned} \tag{14}$$

and $d_{T_x} = d_T\cos\theta_T\cos\psi_T$, $d_{T_y} = d_T\sin\theta_T\cos\psi_T$, $d_{R_x} = d_R\cos\theta_R\cos\psi_R$, and $d_{R_y} = d_R\sin\theta_R\cos\psi_R$.

Many existing correlation functions are special cases of the 3-D MIMO M-to-M space-time correlation function in (13). The simplest special case of (13) is Clark's temporal correlation function $J_0(2\pi f_{R\max}\tau)$ [15], obtained for $k_R = \beta_{R_m} = 0$ (2-D isotropic scattering around $\mathrm{R_x}$), $f_{T\max} = k_T = 0$ (stationary $\mathrm{T_x}$, no scattering), and $d_T = d_R = 0$ (single-antenna $\mathrm{T_x}$ and $\mathrm{R_x}$), where $J_0(\ \cdot\ )$ is the first kind zeroth-order Bessel function. Expressions for other space-time correlation functions based on the "one-ring" model [16], [17], and based on the "one-cylinder" model [11], [18] can be similarly obtained. The temporal correlation function for M-to-M channels, assuming 2-D isotropic scattering, $J_0(2\pi f_{T\max}\tau)J_0(2\pi f_{R\max}\tau)$ [1], is obtained for $k_T = k_R = 0$, $d_T = d_R = 0$, and $\beta_{T_m} = \beta_{R_m} = 0$. Finally, the space-time correlation function for M-to-M channels, assuming 2-D non-isotropic scattering, $I_0(\sqrt{x^2+y^2})I_0(\sqrt{z^2+w^2})/(I_0(k_T)I_0(k_R))$ [7] is obtained for $\beta_{T_m} = \beta_{R_m} = 0$.

V. Sum-of-Sinusoids Simulation Models

The reference model described in Section III assumes an infinite number of scatterers, which prevents practical implementation. Here, we propose a simulation model having a finite number of scatterers that closely matches the statistical properties of the reference model.

Using the reference model and assuming 3-D non-isotropic scattering, the following function is considered for the received complex faded envelope:

$$\begin{aligned} h_{pq}(t) &= \frac{1}{\sqrt{MN}} \sum_{m=1}^{M} \sum_{n=1}^{N} a_{p,m} b_{n,q} \exp\{j\phi_{mn}\} \\ &\times \exp\Big\{j2\pi t\Big[f_{T\max}\cos\left(\alpha_T^{(m)} - \gamma_T\right)\cos\beta_T^{(m)} \\ &+ f_{R\max}\cos\left(\alpha_R^{(n)} - \gamma_R\right)\cos\beta_R^{(n)}\Big]\Big\}, \end{aligned} \tag{15}$$

where parameters $a_{p,m}$ and $b_{n,q}$ are defined in (6) and (7). The angles of departure, $\alpha_T^{(m)}$ and $\beta_T^{(m)}$, and the angles of arrival, $\alpha_R^{(n)}$ and $\beta_R^{(n)}$, are random variables and the angles of departure are independent from the angles of arrival. The phases ϕ_{mn} are also random variables uniformly distributed on the interval $[-\pi, \pi)$ and independent from the angles of departure and the angles of arrival. The AAoDs, $\alpha_T^{(m)}$, and the AAoAs, $\alpha_R^{(n)}$, are modelled using the von Mises pdfs $f(\alpha_T) = \exp[k_T\cos(\alpha_T - \mu_T)]/(2\pi I_0(k_T))$ and $f(\alpha_R) =$

$\exp\left[k_R \cos(\alpha_R - \mu_R)\right]/(2\pi I_0(k_R))$, respectively. They are generated as follows:

$$\alpha_T^{(m)} = F_T^{-1}(\eta_m), \quad \alpha_R^{(n)} = F_R^{-1}(\delta_n), \tag{16}$$

for $m = 1, \ldots, M$, $n = 1, \ldots, N$. Function $F_{T/R}(\ \cdot\ )^{-1}$ denotes the inverse function of the von Mises cumulative distribution function (cdf) and can be evaluated using method in [19]. Parameters η_m and δ_n are independent random variables uniformly distributed on the interval $(0, 1)$. The EAoDs, $\beta_T^{(m)}$, and the EAoAs, $\beta_R^{(n)}$, are modelled using the pdfs $f(\beta_T) = \pi\cos(\pi\beta_T/(2\beta_{T_m}))/(4|\beta_{T_m}|)$ and $f(\beta_R) = \pi\cos(\pi\beta_R/(2\beta_{R_m}))/(4|\beta_{R_m}|)$, respectively, and are generated as follows:

$$\beta_T^{(m)} = \frac{2\beta_{T_m}}{\pi}\arcsin(2\nu_m - 1), \tag{17}$$

$$\beta_R^{(n)} = \frac{2\beta_{R_m}}{\pi}\arcsin(2\zeta_n - 1), \tag{18}$$

for $m = 1, \ldots, M$, $n = 1, \ldots, N$, where parameters ν_m and ζ_n are independent random variables uniformly distributed on the interval $(0, 1)$.

For the maximum elevation angles β_{T_m} and β_{R_m} in the range $1^\circ \leq |\ \beta_{T_m}, \beta_{R_m}\ | \leq 20^\circ$, all random variables in (15), i.e., $\alpha_T^{(m)}$, $\alpha_R^{(n)}$, $\beta_T^{(m)}$, $\beta_R^{(n)}$, and ϕ_{mn}, can be treated as mutually independent random variables and the elevation angles can be approximated using $\cos\beta_T^{(m)}, \cos\beta_R^{(n)} \approx 1$, $\sin\beta_T^{(m)} \approx \beta_T^{(m)}$, and $\sin\beta_R^{(n)} \approx \beta_R^{(n)}$. Then, the complex faded envelope in (15) can be approximated as

$$\begin{aligned} h_{pq}(t) \approx\ & \frac{1}{\sqrt{M_A M_E N_A N_E}} \sum_{m,i=1}^{M_A, M_E} \sum_{n,k=1}^{N_A, N_E} c_{p,m,i} d_{n,k,q} \\ \times\ & \exp\left\{ j2\pi t \left[f_{T\max}\cos\left(\alpha_T^{(m)} - \gamma_T\right) \right.\right. \\ +\ & \left.\left. f_{R\max}\cos\left(\alpha_R^{(n)} - \gamma_R\right)\right] + j\phi_{m,i,n,k} \right\}, \end{aligned} \tag{19}$$

where $M_A M_E = M$, $N_A N_E = N$ and parameters $c_{p,m,i}$ and $d_{n,k,q}$ are defined as

$$\begin{aligned} c_{p,m,i} = \exp\Bigg\{ & j\frac{2\pi}{\lambda} d_T \left[\cos\psi_T \cos\theta_T \cos\alpha_T^{(m)} \right. \\ & \left. + \cos\psi_T \sin\theta_T \sin\alpha_T^{(m)} + \sin\psi_T \sin\beta_T^{(i)} \right] \Bigg\}, \end{aligned} \tag{20}$$

$$\begin{aligned} d_{n,k,q} = \exp\Bigg\{ & j\frac{2\pi}{\lambda} d_R \left[\cos\psi_R \cos\theta_R \cos\alpha_R^{(n)} \right. \\ & \left. + \cos\psi_R \sin\theta_R \sin\alpha_R^{(n)} + \sin\psi_R \sin\beta_R^{(k)} \right] \Bigg\}. \end{aligned} \tag{21}$$

First, we propose an ergodic statistical (deterministic) model. This model has only phases $\phi_{m,i,n,k}$ as random variables and needs only one simulation trial to obtain the desired statistical properties. We use the complex faded envelope in (19) and generate the AAoDs, the AAoAs, the EAoDs, and the EAoAs as follows:

$$\alpha_T^{(m)} = F_T^{-1}\left(\frac{m - 0.5}{M_A}\right), \tag{22}$$

$$\alpha_R^{(n)} = F_R^{-1}\left(\frac{n - 0.5}{N_A}\right), \tag{23}$$

$$\beta_T^{(i)} = \frac{2\beta_{T_m}}{\pi}\arcsin\left(\frac{2i - 1}{M_E} - 1\right), \tag{24}$$

$$\beta_R^{(k)} = \frac{2\beta_{R_m}}{\pi}\arcsin\left(\frac{2k - 1}{N_E} - 1\right), \tag{25}$$

for $m = 1, \ldots, M_A$, $n = 1, \ldots, N_A$, $i = 1, \ldots, M_E$, $k = 1, \ldots, N_E$, respectively. The function $F_{T/R}^{-1}(\ \cdot\ )$ is the inverse function of the von Mises cdf and is evaluated using method in [19].

For $M, N \to \infty$, our deterministic model can be shown to exhibit properties of the reference model [20]. The space-time correlation function of the complex faded envelope in (19) matches the approximated space-time correlation function in (13).

Fig. 2 shows the space-time correlation function ($d_T = d_R = 1\lambda$) of the deterministic model for a linear antenna array with $L_t = L_r = 2$ antennas, using $M_A = 45$, $M_E = 5$, $N_A = 45$, and $N_E = 5$ scatterers. Other parameters used to obtain the curves in Fig. 2 are $\theta_T = \theta_R = \pi/3$, $\psi_T = \psi_R = \pi/4$, $\gamma_T = \pi/6$, $\gamma_R = \pi/12$, $\beta_{T_m} = \beta_{R_m} = 15^\circ$, $k_T = k_R = 2$, and $\mu_T = \mu_R = \pi/4$. Results show that the space-time correlation function of the deterministic model closely matches the theoretical one in the range of normalized time delays, $0 \leq f_{T\max} T_s \leq 4$.

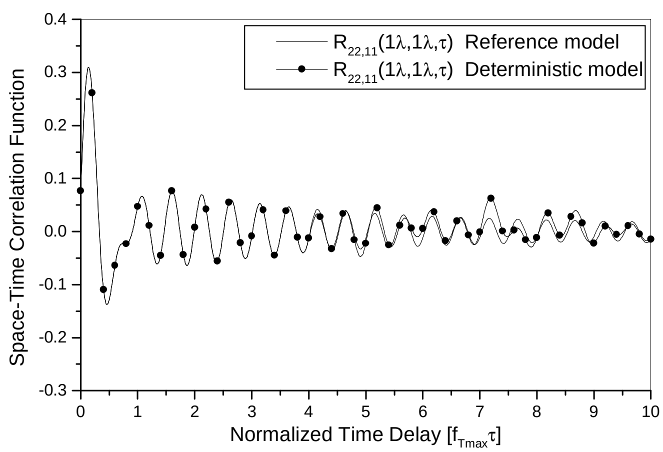

Fig. 2. The normalized space-time correlation function ($d_T = d_R = 1\lambda$) of the complex faded envelope of the deterministic and reference models.

By allowing phases and Doppler frequencies to be random variables, our deterministic model can be modified to match statistical properties of the reference model over a wider range of normalized time delays, while at the same time requiring a smaller number of scatterers. The statistical properties of this (statistical) model vary for each simulation trial, but will converge to desired ensemble averaged properties when averaged over a sufficient number of simulation trials. The complex faded envelope is defined in (19) and the AAoDs, the

AAoAs, the EAoDs, and the EAoAs are generated as follows:

$$\alpha_T^{(m)} = F_T^{-1}\left(\frac{m+\theta_A-1}{M_A}\right), \quad (26)$$

$$\alpha_R^{(n)} = F_R^{-1}\left(\frac{n+\psi_A-1}{N_A}\right), \quad (27)$$

$$\beta_T^{(i)} = \frac{2\beta_{T_m}}{\pi}\arcsin\left(\frac{2(i+\theta_E-1)}{M_E}-1\right), \quad (28)$$

$$\beta_R^{(k)} = \frac{2\beta_{R_m}}{\pi}\arcsin\left(\frac{2(k+\psi_E-1)}{N_E}-1\right), \quad (29)$$

for $m = 1, \ldots, M_A$, $n = 1, \ldots, N_A$, $i = 1, \ldots, M_E$, $k = 1, \ldots, N_E$, respectively. The parameters θ_A, ψ_A, θ_E, and ψ_E are independent random variables uniformly distributed on the interval $[0, 1)$. The function $F_{T/R}^{-1}(\ \cdot\ )$ is the inverse function of the von Mises cdf and is evaluated using method in [19].

Fig. 3 shows the space-time correlation function ($d_T = d_R = 1\lambda$) of the statistical model for a linear antenna array with $L_t = L_r = 2$ antennas, using $M_A = 20$, $M_E = 3$, $N_A = 20$, and $N_E = 3$ scatterers and $N_{\mathrm{stat}} = 50$ simulation trials. Other parameters are the same as in Fig. 2. Results show that the space-time correlation function of the statistical model closely matches the theoretical one in the wider range of normalized time delays, $0 \le f_{T\max} T_s \le 10$.

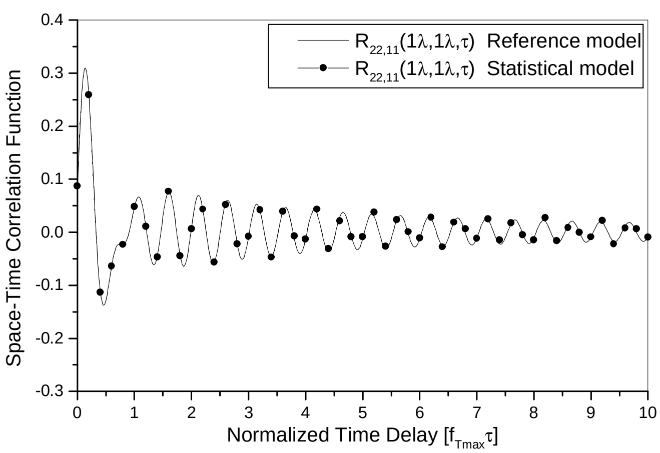

Fig. 3. The normalized space-time correlation function ($d_T = d_R = 1\lambda$) of the complex faded envelope of the statistical and reference models.

VI. Conclusions

In this paper, a two-cylinder geometrical propagation model is introduced. Based on this geometrical model, a 3-D reference model for MIMO M-to-M fading channels is proposed. From the reference model, a closed-form joint space-time correlation function for 3-D non-isotropic scattering environment can be derived. Many existing correlation functions in the literature are special cases of our 3-D MIMO M-to-M space-time correlation function. Finally, deterministic and statistical SoS simulators are presented and shown to closely match the statistical properties of the reference model.

Disclaimer

The views and conclusions contained in this document are those of the authors and should not be interpreted as representing the official policies, either expressed or implied, of the Army Research Laboratory or the U. S. Government.

References

[1] A.S. Akki and F. Haber, “A statistical model for mobile-to-mobile land communication channel,” *IEEE Trans. on Veh. Tech.*, vol. 35, pp. 2–10, Feb. 1986.

[2] A.S. Akki, “Statistical properties of mobile-to-mobile land communication channels,” *IEEE Trans. on Veh. Tech.*, vol. 43, pp. 826–831, Nov. 1994.

[3] R. Wang and D. Cox, “Channel modeling for ad hoc mobile wireless networks,” *Proc. IEEE Veh. Tech. Conf.*, vol. 1, pp. 21–25, Birmingham, AL, May 2002.

[4] C.S. Patel, G.L. Stüber, and T. G. Pratt, “Simulation of Rayleigh-faded mobile-to-mobile communication channels,” *IEEE Trans. on Commun.*, vol. 53, pp. 1876–1884, Nov. 2005.

[5] A.G. Zajić and G.L. Stüber, ”A new simulation model for mobile-to-mobile Rayleigh fading channels,” *Proc. IEEE WCNC’06*, Las Vegas, NE, USA, April 2006.

[6] M. Pätzold, B.O. Hogstad, N. Youssef, and D. Kim, “A MIMO mobile-to-mobile channel model: Part I-the reference model,” *Proc. IEEE PIMRC’05*, vol. 1, pp. 573–578, Berlin, Germany, Sept. 2005.

[7] A.G. Zajić and G.L. Stüber, ”Space-Time Correlated MIMO Mobile-to-Mobile Channels,” *Proc. IEEE PIMRC’06*, Helsinki, Finland, Sept. 2006.

[8] B.O. Hogstad, M. Pätzold, N. Youssef, and D. Kim, “A MIMO mobile-to-mobile channel model: Part II-the simulation model,” *Proc. IEEE PIMRC’05*, vol. 1, pp. 562–567, Berlin, Germany, Sept. 2005.

[9] A.G. Zajić and G.L. Stüber, ”Simulation Models for MIMO Mobile-to-Mobile Channels,” *Proc. IEEE MILCOM’06*, Washington, D.C., USA, Oct. 2006.

[10] T. Aulin, “A modified model for the fading at a mobile radio channel,” *IEEE Trans. on Veh. Tech.*, vol. VT–28, pp. 182–203, 1979.

[11] J.D. Parsons and A.M.D. Turkmani, “Characterisation of mobile radio signals: model description,” *IEE Proc. I, Commun., Speach, and Vision*, vol. 138, pp. 549–556, Dec. 1991.

[12] A. Abdi, J.A. Barger, and M. Kaveh, ”A parametric model for the distribution of the angle of arrival and the associated correlation function and power spectrum at the mobile station,” *IEEE Trans. on Veh. Tech.*, vol. 51, pp. 425–434, May 2002.

[13] Y. Yamada, Y. Ebine, and N. Nakajima, “Base station/vehicular antenna design techniques employed in high capacity land mobile communications system,” *Rev. Elec. Commun. Lab.*, NTT, pp. 115–121, 1987.

[14] A.G. Zajić and G.L. Stüber, ”A Three-Dimensional MIMO Mobile-to-Mobile Channel Model,” to appear in *IEEE WCNC’07*, Hong Kong, March 2007.

[15] R.H. Clarke, “A statistical theory of mobile-radio reception,” *Bell Syst. Tech. J.*, pp. 957–1000, July–Aug. 1968.

[16] D. Shiu, G.J. Foschini, M.J. Gans, and J.M. Khan, ”Fading correlation and its effect on the capacity of multielement antenna systems,” *IEEE Trans. on Commun.*, vol. 48, pp. 502–513, Mar. 2000.

[17] A. Abdi and M. Kaveh, ”A space-time correlation model for multielement antenna systems in mobile fading channels,”*IEEE J. Select. Areas in Commun.*, vol. 20, pp. 550–560, Apr. 2002.

[18] S.Y. Leong, Y.R. Zheng, and C. Xiao, “Space-time fading correlation functions of a 3-D MIMO channel model,” *Proc. IEEE WCNC’04*, vol. 2, pp. 1127–1132, Atlanta, GA, Mar. 2004.

[19] K. V. Mardia and E. P. Jupp, *Directional Statistics*. New York. Wiley 1999.

[20] A.G. Zajić and G.L. Stüber, ”Three-Dimensional Modelling, Simulation and Capacity Analysis of Space-Time Correlated Mobile-to-Mobile Channels,” submitted to *IEEE Transactions on Vehicular Technology*.